

Internally Cured High Performance Concrete with Magnesium based Expansive Agent using Coal Bottom Ash Particles as Water Reservoirs

Roberto Rodríguez-Álvaro¹, B. González-Fonteboa^{1*}, S. Seara-Paz¹, Khandaker M.A. Hossain²

¹*Department of Civil Engineering, Campus de Elviña s/n, 15071 A Coruña, Universidade da Coruña, Spain.*

roberto.rodriguez1@udc.es ; bfonteboa@udc.es ; gumersinda.spaz@udc.es

²*Department of Civil Engineering, Ryerson University, 350 Victoria St., Toronto, ON, M5B 2K3, Canada*

ahossain@ryerson.ca

*Corresponding author: bfonteboa@udc.es

Abstract

Shrinkage is one of the main concerns related to high performance concrete (HPC) durability. Its high density paste, consequence of a low water to binder ratio, can be unprofitable if cracks appear due to excessive tension when volume changes are restrained. Therefore, volume stability is a priority. In this work, three different strategies have been studied with that purpose: integration of fly ash as a low reactive supplementary cementitious material, internal curing via coal bottom ash particles as water reservoirs and the use of an expansive agent based on magnesium oxide (MEA). Many research works address the three shrinkage reduction strategies individually. However, studies regarding their simultaneous use are not prevalent so this work proposes its combined application. Results indicate that internal curing and MEA have a synergistic effect in HPC. Internal curing enhances MEA expansion due to the lack of water in this kind of concrete, contributing to autogenous shrinkage compensation. When concrete is affected by air-drying conditions, the use of MEA, internal curing, or both together make shrinkage to increase. MEA effectively expands in wet cured HPC although internal curing is not effective in this condition due to the absence of self-desiccation and limited porous aggregate water desorption. Taking into account the effects of each shrinkage reduction strategy and curing condition, it has been concluded that the use of fly ash as supplementary cementitious material, internal curing and MEA is recommended together with prevention of water evaporation from HPC surface.

31 **Keywords:** Fly Ash; Magnesium based Expansive Agent; Coal Bottom Ash; Internal Curing;
32 Autogenous shrinkage; Drying shrinkage; Swelling.

33

34

35 **Highlights:**

- 36 • Three shrinkage reduction strategies were used in high performance concrete (HPC)
- 37 • Internal curing water can contribute to magnesium expansive agent (MEA) hydration
- 38 • MEA makes shrinkage to increase in HPC affected by air-drying curing conditions
- 39 • [MEA hydration product, magnesium hydroxide, carbonates on concrete surface](#)

40 **1. Introduction and objectives**

41 Volume stability is a remarkable issue that must be taken into account when designing concrete for
42 structural and non-structural applications. Different phenomena can make concrete to suffer deformations,
43 generating internal stress if they are constrained. This tension can exceed tensile strength and produce
44 cracks letting potentially harmful agents to ingress concrete. Therefore, concrete shrinkage can lead to
45 important durability problems [1].

46 Concrete deformations can be positive (volume increase, i.e. swelling or expansion) or negative (volume
47 reduction, i.e. shrinkage) and some of them can be absent depending on concrete composition and
48 surrounding environmental conditions. Concrete external volume changes are known as autogenous
49 deformations when they are intrinsic to material's composition, no matter surrounding conditions. These
50 kind of deformations can increase (autogenous swelling) or reduce (autogenous shrinkage) concrete
51 volume as a consequence of different physical and chemical processes.

52 Cement hydration provokes an external volume reduction before setting, and it is the driving force of
53 autogenous shrinkage after setting. Concrete internal relative humidity decreases due to cement hydration
54 and other supplementary cementitious materials reactions that consume water, such as pozzolanic
55 reactions [2]. This progressive process is named as self-desiccation and, when intense enough, it is the
56 cause of autogenous shrinkage [3–5]. Therefore, self-desiccation is a special concern in concrete with a
57 low water to cement ratio, i.e. high performance concrete (HPC) [3,6,7]. Cement hydration rate becomes
58 lower as time goes by. Therefore, autogenous shrinkage is more remarkable during the first days after
59 concrete mixing. However, an opposite deformation can compensate self-desiccation shrinkage at early
60 ages. That is autogenous swelling and can be caused by different phenomena such as absorption of
61 bleeding water, water adsorption by fillers, CH growth and primary ettringite formation [8,9]. Also, some
62 recent approaches to the effect of cement hydration on a porous-system scale state that C-S-H formation
63 decisively contributes to swelling as long as a sufficient relative humidity is maintained inside concrete
64 [10,11]. Sometimes, autogenous swelling cannot be observed as it coexists with autogenous shrinkage in
65 a minor magnitude, resulting an overall negative deformation [12]. That is one of the possible reasons for

66 it to be less studied [13] although it plays an important role in shrinkage compensation and cracking
67 prevention at early ages [14].

68 Cement hydration is also the direct cause of thermal deformations, as it is an exothermic reaction. Heat
69 of hydration makes concrete temperature to rise to a peak and then decrease, causing associated
70 expansion and shrinkage. The magnitude of this temperature change depends on the rate of heat
71 dissipation into the surrounding environment. This is why thermal deformations should not be considered
72 autogenous.

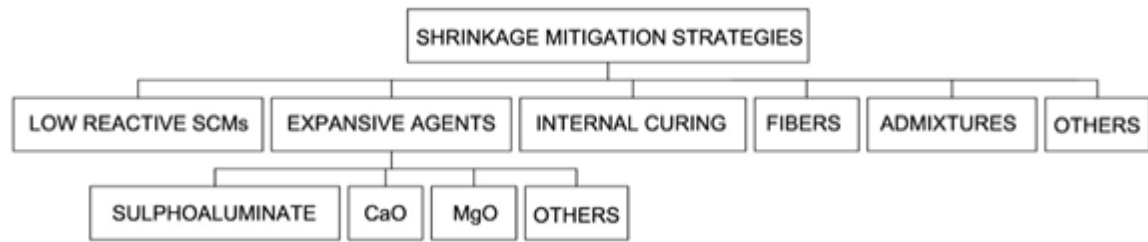
73 When interaction of concrete with the environment is allowed, the moisture gradient forces unbound
74 water to evaporate. Then, water migration from the capillary pores to the outside develops pressure on
75 them and a volume reduction occurs. This mechanism is analogous to the one that governs self-
76 desiccation [15]. High water to cement ratios and low environmental humidity increase drying shrinkage
77 [16,17]. Drying shrinkage magnitude is related to specimens shape and size, as water release is not
78 homogeneous across specimen's cross section [14,18–20].

79 On the opposite direction, from environment to concrete, there is another element that migrates: CO₂.
80 Carbon dioxide is naturally present on air and can react with calcium based concrete compounds, mainly
81 calcium hydroxide formed as a product of Portland cement hydration. This carbonation implies a volume
82 reduction known as carbonation shrinkage, which is not completely understood yet [21].

83 All previously mentioned deformations can coexist in laboratory samples and construction elements,
84 depending on their size, shape and surrounding environment. Different strategies can be used in order to
85 mitigate them [2]: low reactive supplementary cementitious materials [22–25], internal restraint by fibre
86 reinforcement [26–28], internal curing [29–32], shrinkage reducing additives (SRA) [33–35] and
87 expansive agents [36–38] are among the most popular [39].

88 Some of these shrinkage reduction strategies are gathered in **Fig. 1**.

89



90

91 **Fig. 1:** Shrinkage reduction strategies.

92 Regarding expansive agents, the most known are based on calcium sulphoaluminate (C- \bar{S} -A) [38,40,41],
 93 calcium oxide (CaO) [42–49] and magnesium oxide (MgO). These expansive agents hydrate resulting in
 94 new compounds with a higher volume. The calcium sulphoaluminate can give rise to ettringite or
 95 monosulfate, with respective volumes of 9.3 and 4.1 times the initial C- \bar{S} -A particle [50]. Calcium oxide
 96 gives rise to calcium hydroxide, with a volume of 1.9 times CaO [50]. Finally, magnesium oxide gives
 97 rise to magnesium hydroxide, with a volume of 2.2 times MgO [51]. However, hydration is not the only
 98 important factor regarding the expansive process. Formation of surrounding hydrates subjected to the
 99 compressive forces produced by the expansive ingredients plays also an important role [50]. The effect of
 100 the use of expansive agents on compressive strength and tightness is strongly related to curing conditions
 101 and especially with restraining extent. Some studies conclude that restrained concrete maintains the
 102 values for these properties when including expansive agents into the mix, while some “loosening” can
 103 happen when no restrictions are applied, causing small decreases of compressive strength and tightness
 104 [50]. This must be taken into account when studying expansive agents’ performance in small non-
 105 restrained laboratory specimens, as results can differ for reinforced structural elements.

106 Magnesium oxide is present in Portland cement as dead burnt periclase, coming mostly from impurities of
 107 magnesite in calcite used as raw material for its manufacturing. In this case, magnesite is submitted to a
 108 temperature over 1400 °C, producing low reactive a kind of magnesia that is only able to expand after
 109 long periods of time. This can cause cracks and associated durability problems [51]. However,
 110 magnesium oxide can be obtained from less intense burning (lightly burnt MgO), which is able to expand
 111 at relatively early ages. **Eq. 4** represents the involved chemical reaction in MgO manufacturing process:



112 Lightly burnt MgO has been proved to be convenient for compensating autogenous shrinkage [52–54],
113 thermal shrinkage in laboratory [55,56] and field conditions [57], and it even shows self-healing capacity
114 [52,58,59]. The expansive mechanism involves hydration of MgO, producing magnesium hydroxide (also
115 known as brucite), with a much higher molar solid volume (117 % bigger than MgO) [51]. **Eq. 5**
116 represents this chemical reaction. Kinetics of MgO dissolution are extendedly explained in [60].



117 Research about lightly burnt MgO started when it was reported that no cracks were formed due to thermal
118 shrinkage in Baishan concrete arch gravity dam in China. This fact was attributed to the use of a Portland
119 Cement with high content of magnesia burnt at a lower than usual temperature [61]. Since then,
120 intentionally lightly burnt MgO has been used to fabricate expansive agents known as magnesium based
121 expansive agents (MEA). Most common MEAs have a high content of magnesium oxide, as they are
122 obtained from pure magnesite extracted in quarries. Less effective but more sustainable and cheap MEA,
123 with less content of MgO, can be obtained from impure magnesite or industrial wastes too [62–64].

124 When comparing MEA with calcium and ettringite based expansive agents, the main advantages are its
125 relatively low need of water to react and the stability of the reaction product, magnesium hydroxide [53].
126 Positive effects of MEA on other durability properties more than shrinkage have been reported [65,66]
127 and also on mechanical properties under restrain condition [67].

128 Supplementary cementitious materials have a remarkable influence on autogenous and thermal stress,
129 tending to reduce those parameters when they are low reactive. For instance, class F fly ash is frequently
130 included in concrete with MEA [37,53,55–57,59,65,66,68,69], working both elements in favour of
131 volume stability. Blended cements containing MEA, especially with class F fly ash, have been widely
132 studied and used for construction of massive dams in China [70].

133 An alternative strategy that can make autogenous shrinkage to decrease is internal curing. This consists in
134 the supply of water to a cementitious mixture using pre-wetted lightweight aggregate, or other materials
135 that readily release water from within particles, thereby mitigating self-desiccation and sustaining
136 hydration [71]. These pre-wetted particles are also known as water reservoirs. Lightweight aggregates and

137 superabsorbent polymers are the most common elements used as water reservoirs [30]. Internal curing is
138 especially useful in high performance concrete, with a very low water to binder ratio. Water in HPC is
139 hardly available for cement hydration, and additional amounts cannot be effectively provided by external
140 curing due to paste low permeability [31]. The use of MEA does not seem a good option for this kind of
141 concrete, as it needs a certain amount of water to react. However, the simultaneous utilization of internal
142 curing and MEA could be a promising combination, as the former could provide the latter with the
143 necessary water to expand. Only a few studies have explored this option [36].

144 **2. Research significance**

145 Worries about HPC early age volume stability have motivated the publication of many papers about
146 shrinkage reduction strategies. However, the most of these research works address each strategy
147 individually. Studies about their combined effect are not prevalent, although this perspective is also
148 interesting because of potential synergistic effects. In addition, the proposal of more than one strategy in
149 order to avoid any concrete dysfunction is usually convenient as they all can present some drawbacks (not
150 only from a technical perspective, but also economical, ecological...). This is the case of the three
151 shrinkage reduction strategies proposed in this study: the use of fly ash as low reactive supplementary
152 cementitious material, internal curing via saturated coal bottom ash as water reservoirs and a magnesium
153 based expansive agent. Synergistic effects have been found and negative consequences of the use of each
154 of them can be minimized when reducing the amount of each of them in favour of a multi-constituent
155 approach. Moreover, three laboratory curing conditions have been established in this study with the aim of
156 getting information about the performance of the materials under study on a real field situation. The
157 authors conclude that HPC with high volume of fly ash, MEA and internal curing is volumetrically more
158 stable than conventional HPC and shows an acceptable strength.

159 **3. Materials characterization and mix design**

160 All materials have a particle size below 4 mm. Therefore, the object of the experimental programme is the
161 mortar phase of a hypothetical HPC. Designed mixes do not contain coarse aggregates but only fine
162 aggregates and paste constituents.

163 Coal bottom ash particles (CBA) have been used as water reservoirs for internal curing. CBA is a porous
 164 granular waste generated in coal power stations. As internal curing affects a wider volume of paste when
 165 using small size water reservoirs [72], CBA particles were sieved to reach a 4 mm maximum size. Some
 166 photographs of different size CBA fractions are shown in **Fig. 2**.

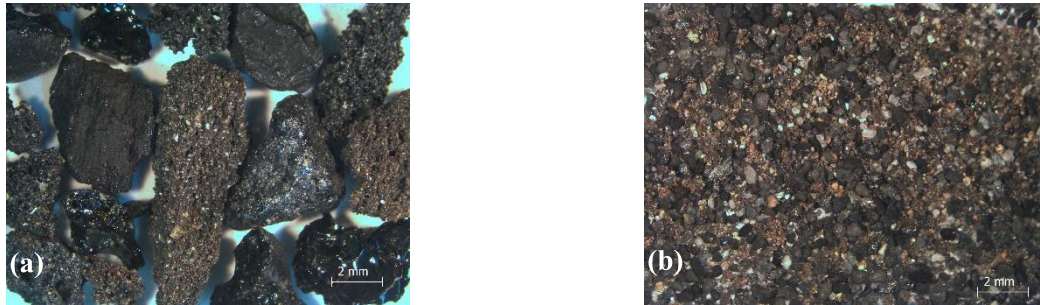


Fig. 2: CBA with a particle size between 2 and 4 mm (a). CBA with a particle size between 0.125 and 0.5 mm (b)

167 Sieved CBA has a dry-state density of 1.19 g/cm³ and a 24 h water absorption of 36.66 %. This element
 168 partially replaces conventional sand (S) in designed mortars, which is crushed sand with a maximum size
 169 of 4 mm, a dry-state density of 2.47 g/cm³ and a water absorption of 2.43 % after 24 h. Both granular
 170 materials present a similar particle size distribution and fineness modulus, being 2.33 for CBA and 2.78
 171 for conventional sand.

172 Ordinary Portland cement (OPC) with a density of 3.12 g/cm³ and Class F fly ash (FA) with a density of
 173 2.21 g/cm³ have been used as the main powder paste constituents. A magnesium based expansive agent
 174 (MEA) has been used in this study. It was obtained by calcination of pure magnesite (see composition in
 175 **Table 1**) with a maximum particle size of 100 μm at 900 °C during 2 h (light burning) as it was done in
 176 previous works by Sherir et al. [59]. Other authors have also deeply studied the influence of different
 177 parameters of the calcining process over MEA performance [69,73]. Small samples of 2.7 kg, divided into
 178 three different containers, were burnt at a time to guarantee a homogeneous calcination (up to an average
 179 lost on ignition of 34 %). The resulting powder compound is basically magnesium oxide (MgO), with a
 180 purity of 90 % and a density of 3.58 g/cm³.

181 **Table 1:** Magnesium carbonate chemical composition

CaO	SiO ₂	Al ₂ O ₃	Fe ₂ O ₃	MgO	LOI
0.46 %	4.17 %	0.52 %	0.49 %	46.72 %	47.21 %

182 After burning, containers were carefully taken out of the kiln and MEA was spread on aluminium trays to
183 ensure a quick temperature drop of the material. After a cooling time of 15 min, MEA was kept in glass
184 jars inside a sealed box containing soda lime and silica gel, which are granular materials with a high water
185 vapour absorption capacity. The cooling procedure is very important as magnesium oxide is an unstable
186 compound that can easily react with environmental humidity. Some stages of this process can be seen in
187 **Fig. 3.**



Fig. 3: MEA obtaining process: taking out from the kiln, pouring and spreading on trays and packing.

188 A high range water reducing admixture (HRWRA) with a $1.05 \pm 0,02 \text{ g/cm}^3$ density and solid residue of
189 $20.3 \pm 1 \%$ has been used in order to enhance fluidity of HPC mortar phase.

190 Taking into account the shown characteristics of each material involved in the study, twelve different
191 HPC mortar phase mixes were designed. The next criteria were considered to establish the mix design:

192 - One half of the mixes contain CBA as internal curing water reservoirs. This material is introduced in
193 the mortar substituting the 30 % of conventional sand (S), by volume.

194 - Two different binders are used: Ordinary Portland cement (OPC) and blended cement (BC). BC is
195 obtained by mixing a 40 % of OPC with a 60 % of FA, proportioned on a volume basis.

196 - Two different MEA contents are established: 3 % and 5 %. MEA replaces OPC when no FA is in
197 binder, while it substitutes FA in BC mixes. This substitution is carried out by volume in both cases.

198 Mix proportions in relation with mortars nomenclature are described in **Table 2.**

199

200

Table 2: Mortar mixes

NOTATION		GRANULAR MATERIALS			POWDER MATERIALS				
		Ø / IC	S	CBA	CM/BCM	C	FA	Ø / MEA3 / MEA5	MEA
CM SERIES	CM-MEA0		100 %	0 %	CM	100 %	0 %	MEA0	0 %
	CM-MEA3				CM	97 %		MEA3	3 %
	CM-MEA5				CM	95 %		MEA5	5 %
	ICCM-MEA0	IC	70 %	30 %	CM	100 %		MEA0	0 %
	ICCM-MEA3	IC			CM	97 %		MEA3	3 %
	ICCM-MEA5	IC			CM	95 %		MEA5	5 %
BCM SERIES	BCM-MEA0		100 %	0 %	BCM	40 %	60 %	MEA0	0 %
	BCM-MEA3				BCM		57 %	MEA3	3 %
	BCM-MEA5				BCM		55 %	MEA5	5 %
	ICBCM-MEA0	IC	70 %	30 %	BCM		60 %	MEA0	0 %
	ICBCM-MEA3	IC			BCM		57 %	MEA3	3 %
	ICBCM-MEA5	IC			BCM		55 %	MEA5	5 %

201

202 Conventional sand and coal bottom ash were soaked in water during 24 h prior to mixing, with an amount

203 of water equivalent to their 24 h water absorption capacity. Water inside these particles performs as an

204 internal curing agent, so it is referred as internal curing water in conventional sand (ICW-S) and internal

205 curing water in coal bottom ash (ICW-CBA). It must be noted that the amount of ICW-S is much lower

206 than ICW-CBA, as coal bottom ash particles have a much higher water absorption. Therefore, only

207 mortars with CBA are referred as internally cured mortars (ICCM).

208 Mixing water (W) to powder materials ratio in terms of volume remains constant for all mixes. Note that

209 mixing water does not include internal curing water referred in previous paragraph. HRWRA dosage is

210 0.80 % in terms of solid residue/OPC, by volume. Note this dosage is not referred to the sum of all

211 powder materials but only to OPC. HRWRA is dosed as to get a fluid mortar with self-compacting

45 212 behaviour. Mix proportions of resulting mixtures are described in Table 3.

46

47

48 213

49

50 214

51

52

53 215

54

55

56 216

57

58

59 **Table 3:** Mix proportions [kg/m³].

		OPC	FA	MEA	S	ICW-S	CBA	ICW-CBA	W	HRWRA
CM SERIES	CM-MEA0	923	0	0	1112	27	0	0	252	15
	CM-MEA3	896	0	32	1112	27	0	0	252	15
	CM-MEA5	878	0	53	1112	27	0	0	252	15
	ICCM-MEA0	923	0	0	778	19	161	59	252	15
	ICCM-MEA3	896	0	32	778	19	161	59	252	15
	ICCM-MEA5	878	0	53	778	19	161	59	252	15
BCM SERIES	BCM-MEA0	370	393	0	1112	27	0	0	252	6
	BCM-MEA3	370	373	32	1112	27	0	0	252	6
	BCM-MEA5	370	360	53	1112	27	0	0	252	6
	ICBCM-MEA0	370	393	0	1112	19	161	59	252	6
	ICBCM-MEA3	370	373	32	1112	19	161	59	252	6
	ICBCM-MEA5	370	360	53	1112	19	161	59	252	6

217

218 4. Test methods

219 Including MEA in concrete as a separate powder (not previously mixed with other elements in other
220 processes like, for example, cement grinding) demands a longer than usual mixing time [53,61]. Concrete
221 homogeneity when using an expansive agent is vital as irregular expansions may cause differential
222 tensions in paste and consequent damage [68]. Therefore, a 5.5 minutes mixing procedure was chosen,
223 which is considered to be enough for MEA proper dispersion. A planetary 20 litres capacity pan mixer
224 was used.

225 Length and mass change were measured using specimens with dimensions 25x25x285 mm³ (gauge length
226 of 250 mm), according to UNE 80112 [74]. Specimens were exposed to three different curing conditions:
227 sealed with aluminium foil (**Fig. 4**), air-drying in an 50 % RH environment (**Fig. 5**) and water immersion
228 (**Fig. 6**). Temperature was kept constant in all curing environments at 24±2 °C. Length and mass changes
229 were measured from 18 h after casting, when specimens were demoulded. An earlier than conventional
230 demoulding age (specimens for shrinkage test are commonly demoulded 24 h after casting) was chosen to
231 start measurements at a time as close as possible to final setting. Length change at different ages was
232 divided by initial length, obtaining strain (µε), while mass changes were divided by specimens' surface in
233 order to get a unitary mass change (g/m²). Mass results normalization by area is chosen as a criterion
234 based on EN 16322 [75].



Fig. 4: Sealed specimens



Fig. 5: Specimens in air-drying conditions



Fig. 6: Specimens immersed in water

235 Compressive strength was measured on sealed cubic samples with 50 mm side at an early age, 7 days, and
 236 long term, 244 days. This way, information about strength development over time can be obtained.

237 **5. Results and discussion**

238 **5.1 Sealed condition: compressive strength and length change**

239 Long term compressive strength of all mixes with OPC as the only binder reach 65 MPa, and mixes with
 ended cement surpass 40 MPa (**Fig. 7**). These results are considered to be acceptable for a mortar phase
 HPC.

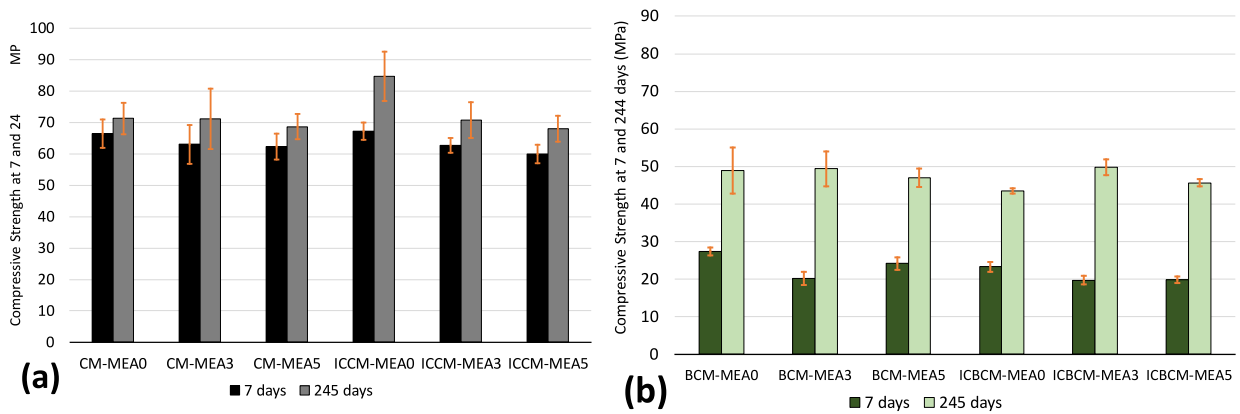


Fig. 7: Compressive Strength of CM (a) and BCM (b) series at 7 and 244 days [MPa]

242 The use of MEA slightly reduces strength of CM mixes because, in these mixes, MEA replaces part of
 243 Portland cement. When blended cement is used, the effect of MEA on strength is not so clear as cement
 244 content remains constant and not all fly ash is expected to have been reacted even at 245 days. Strength
 245 index of mixes with CBA, considering mixes without CBA as reference, slightly varies around 1, being

246 0.89 the minimum (ICBCM-MEA0) and 1.19 the maximum (ICCM-MEA0). Therefore, the effect of the
 247 alternative aggregate on compressive strength can be neglected. As expected, mixes with fly ash gain
 248 strength slowly, reaching about a 50 % of their maximum at 7 days. On the other hand, CM mortars
 249 strengthen faster, achieving the 90 % of their maximum at the same early age.

250 In sealed condition, control mixes without internal curing or MEA show the highest deformation of their
 251 respective series at all times, as can be seen in **Fig. 8**.

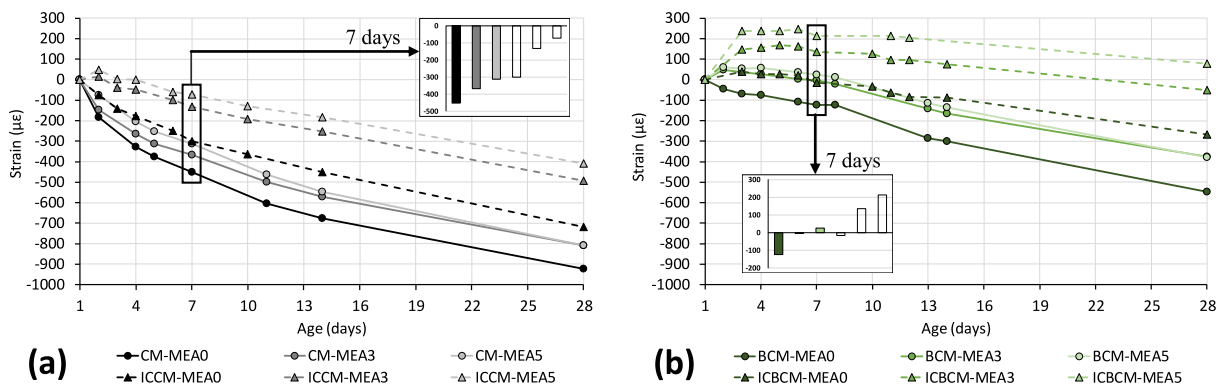


Fig. 8: CM (a) and BCM (b) strain in sealed conditions [$\mu\epsilon$].

252 For some of the mixes, it has been recorded an initial positive deformation which is possibly caused by
 253 swelling due to internal bleeding, i.e. aggregates water desorption, and MEA expansion. Blended cement
 254 internally cured mixes with MEA show the greatest positive deformation (**Table 4**). The lower hydration
 255 activity in BCM mixes consumes less water at early ages, reducing paste self-desiccation and leaving
 256 more water available for MEA hydration. Saturated CBA desorb water (internal bleeding) causing
 257 swelling and enhancing MEA expansion.

Table 4: Swelling peak time (days) and strain ($\mu\epsilon$).

	CM-MEA0	CM-MEA3	CM-MEA5	ICCM-MEA0	ICCM-MEA3	ICCM-MEA5
Time	-	-	-	-	2	2
Value	-	-	-	-	16	18
	BCM-MEA0	BCM-MEA3	BCM-MEA5	ICBCM-MEA0	ICBCM-MEA3	ICBCM-MEA5
Time	-	2	2	3	5	6
Value	-	48	62	40	168	246

258

259 After the swelling peak, shrinkage starts. In sealed curing condition, with no moisture exchange with the
 260 environment, recorded shrinkage is autogenous shrinkage. In **Fig. 9**, Swelling has been removed from the
 261 total recorded deformations in order to only analyse autogenous shrinkage. Over time, all mixes maintain
 262 their relative position from the one with the highest shrinkage to the one with the lowest.

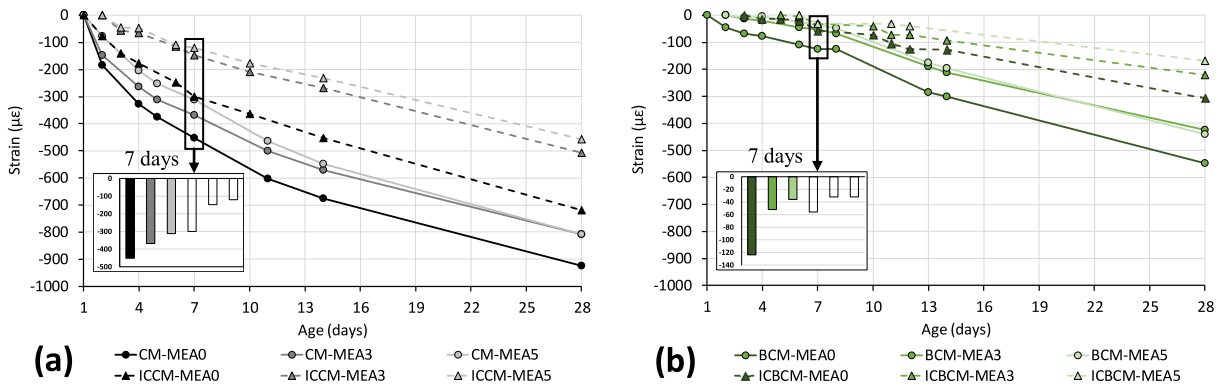


Fig. 9: CM (a) and BCM (b) autogenous shrinkage [$\mu\epsilon$].

263 Autogenous shrinkage is higher for CM specimens than for their BCM counterparts, as less cement
 264 hydration leads to less self-desiccation. Autogenous shrinkage is lower when internal curing is applied, as
 265 it mitigates paste self-desiccation. The positive effect of internal curing is more remarkable during the
 266 first days and remains over time.

267 MEA expansion partially compensates autogenous shrinkage for both CM and BCM series. This effect,
 268 however, is only visible during the first days after demoulding if internal curing is not applied. For that
 269 case, there is no proportional improvement in late autogenous shrinkage (28 days) when increasing the
 270 amount of MEA from 3 to 5 %. CM-MEA3 shows barely the same autogenous shrinkage at 28 days than
 271 CM-MEA5, and there is no significant difference between BCM-MEA3 and BCM-MEA5 either. HPC,
 272 produced with a small amount of mixing water, seems not to be able to provide enough water for MEA to
 273 expand. Some extra water is needed and internal curing can provide it. Proof of this are the improvements
 274 of ICCM-MEA5 over ICCM-MEA3 and of ICBCM-MEA5 over ICBCM-MEA3 (84 and 130 $\mu\epsilon$ at 28
 275 days, respectively). Available water in non-internally cured mixes is not enough even for hydrating all
 276 MEA in mixes with a 3 % content. This is stated after having registered a 228 $\mu\epsilon$ compensation at 28 days
 277 of ICCM-MEA3 over ICCM-MEA0, and a quite inferior, 116 $\mu\epsilon$, of CM-MEA3 over CM. Similar

278 behaviour is found for mortars with fly ash, with a 216 $\mu\epsilon$ compensation of ICBCM-MEA3 over ICBCM-
 279 MEA0, and an inferior one, 171 $\mu\epsilon$, of BCM-MEA3 over BCM. However, this lack of water for proper
 280 MEA hydration in HPC is not detected during the first days after demoulding. At that time, the higher the
 281 MEA content the lower the shrinkage in case of CM series, and the higher the swelling in case of BCM
 282 series.

283 Internal curing is a shrinkage reducing strategy playing a double role in HPC with MEA. It contributes
 284 not only to autogenous shrinkage reduction but also to compensate it by providing extra water for MEA
 285 hydration. This beneficial synergistic effect has been also reported in other works [65].

286 **5.2 Air-drying conditions: mass change and shrinkage**

287 Mortars lose water by evaporation when submitted to air-drying conditions, which can be recorded as
 288 mass loss. Mass loss is especially remarkable during the first days after demoulding and tends to stabilize
 289 at early ages due to high surface to volume ratio of shrinkage specimens, and it even turns into mass gain
 290 after 14 days for BCM series due to carbonation. The described tendency can be observed in **Fig. 10**.

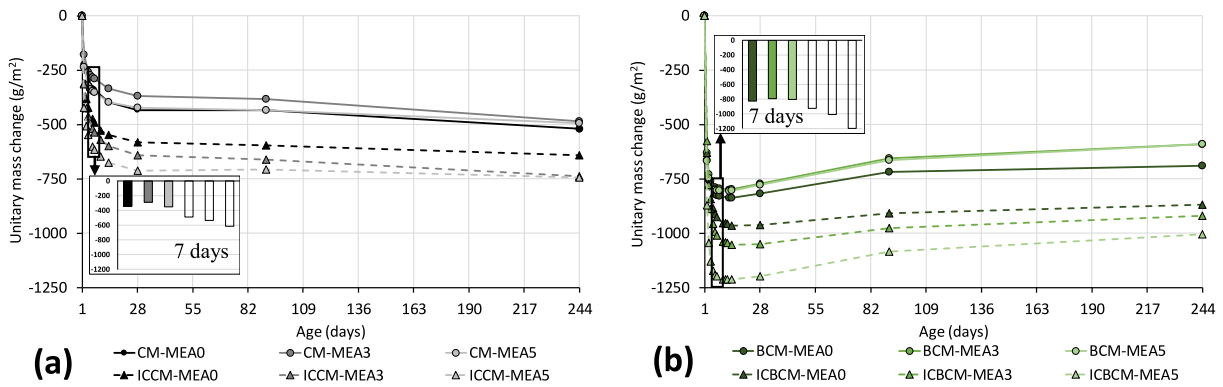


Fig. 10: CM (a) and BCM (b) mass loss in air-drying conditions (g/m²).

291 The initial drastic drop is lower for CM series because they consume more water during setting, when
 292 mortar is still inside the sealed mould. Internally cured mixes have a higher mass loss as they contain a
 293 higher amount of water (ICW-CBA > ICW-S). Presence of MEA increases mass loss in internally cured
 294 specimens in a slight magnitude.

295 As said before, after 14 days, mass gain due to carbonation can be observed in BCM series. Carbon
 296 dioxide fixing capacity is typically lower when pozzolanic materials as fly ash are used due to portlandite
 297 consumption [76]. However, specimens under air-drying conditions have been poorly cured so pozzolanic
 298 reaction might not have taken place properly. Moreover, poorly cured BCM may develop a porous
 299 network that enhances carbon dioxide diffusion, in contrast with CM exposed to the same curing
 300 conditions. This long term tendency is not typically measurable when large specimens are used, but other
 301 studies have registered similar mass gain [5,77,78]. Total mass gain from 14 days onwards can be found
 302 in **Table 5**.

Table 5: Mass gain from 14 to 244 days age (g/m^2).

BCM-MEA0	BCM-MEA3	BCM-MEA5	ICBCM-MEA0	ICBCM-MEA3	ICBCM-MEA5
148	208	214	98	131	207

303

304 This registered mass gain is the result of the combination of CO_2 collection and water evaporation. That is
 305 the reason for internally cured mixes to show a lower mass gain. They still lose a considerable amount of
 306 water after 14 days, higher than their non-internally cured counterparts, because of their higher initial
 307 water content. This effect is also noticeable at the period between 7 and 14 days, when non-internally
 308 cured specimens already show a lower mass loss than the internally cured counterparts. For instance:
 309 BCM-MEA0 loses 11.59 g/m^2 during this time period, while ICBCM-MEA0 loses 39.84 g/m^2 . The mass
 310 gain rhythm due to carbonation is constant when no significant mass loss is simultaneously occurring and
 311 drastically decreases when the carbonation depth reaches the whole specimen (with a small cross section),
 312 i.e. almost all carbonatable compounds have been carbonated. This tendency can be seen in non-internally
 313 cured specimens after 14 days, being the carbonation ending at around 91 days (**Table 6**).

Table 6: Mass gain rhythm ($\text{g/dm}^3 \cdot \text{day}$).

Time period	BCM-MEA0	BCM-MEA3	BCM-MEA5
14 to 28 days	1.59	1.77	1.85
28 to 91 days	1.56	1.88	1.82
91 to 244 days	0.18	0.43	0.48

314

315 This tendency cannot be clearly seen in internally cured mixes for the same period because they lose
 316 water for a longer time. Although mass gain is not clearly observable in CM series, a little amount of
 317 carbonation might coexist with water evaporation. Associated mass changes, positive and negative
 318 respectively, may balance each other resulting a negligible mass loss for this period. After that age,
 319 almost all carbonatable compounds are believed to be carbonated so a small mass loss due to water
 320 evaporation is registered.

321 The presence of MEA means an increase in carbonation mass gain (**Table 5**), as magnesium hydroxide
 322 can react with environmental carbon dioxide to form magnesium carbonate. This mass gain is also faster
 323 when MEA is used, what means it reacts with environmental CO₂ at the same time other compounds
 324 contained in fly ash and Portland cement do. For example, ICBCM-MEA0, ICBCM-MEA3 and ICBCM-
 325 MEA5 gain mass at a ratio of 0.87, 1.16 y 1.78 g/m²·day, respectively, for the time period between 28 and
 326 91 days.

327 In air-drying curing condition, the interactions of mortar with the surrounding environment cause
 328 continuous shrinkage (**Fig. 11**). Along time, all mixes maintain their relative position from the one with
 329 the highest shrinkage to the one with the lowest. Expansions due to MEA are not registered in air-drying
 330 curing conditions. What is more, mortars with MEA show a higher shrinkage.

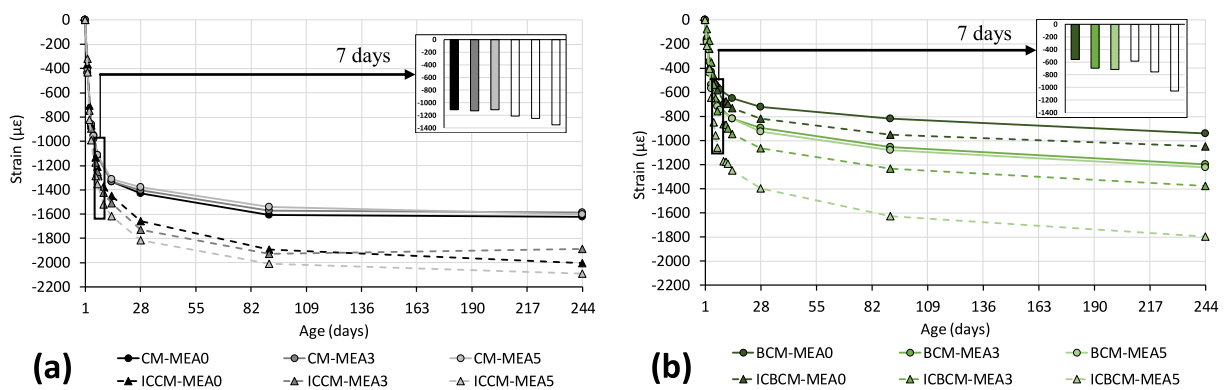
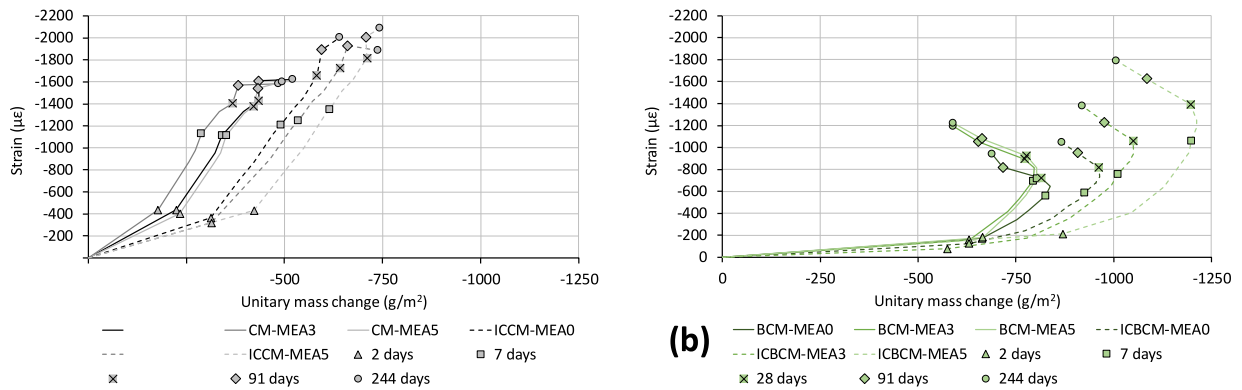


Fig. 11: CM (a) and BCM (b) shrinkage in air-drying conditions [$\mu\epsilon$].

331 Shrinkage increase decelerates over time and CM series show higher values than BCM series. At this
 332 point, doing a quick comparison between **Fig. 10** and **Fig. 11**, it can be clearly observed that CM series
 333 lose less water but show a higher shrinkage than BCM series. This is not the usual correlation between

334 mass loss and shrinkage that can be found in studies about conventional concrete. In HPC and mortars
 335 with a low water to binder ratio, as it is the case of this study, paste self-desiccation coexists with drying
 336 and carbonation in air-drying curing condition. An approach about the importance of each of those
 337 phenomena on total shrinkage can be got by plotting shrinkage against unitary mass change ratio (**Fig.**
 338 **12**).



and BCM **(b)** shrinkage ($\mu\epsilon$) for corresponding unitary mass loss (g/m^2).

day after demoulding (from first record until the age of 2 days), for the same mass loss, there is more shrinkage in non-internally cured specimens than in the internally cured specimens for both CM and BCM series.

BCM-MEA0 has a shrinkage to mass loss ratio of $1.95 \mu\epsilon/(g/m^2)$ at the age of 2 days while

342 the internally cured counterpart has a shrinkage of $1.16 \mu\epsilon/(g/m^2)$. This corroborates that self-desiccation
 343 shrinkage coexists with air-drying shrinkage at early ages, as internal curing is known to mitigate self-
 344 desiccation shrinkage.

345 For CM series, from 28 to 91 days, the possible coexistence of drying and carbonation makes a low mass
 346 loss to cause a relatively high shrinkage. Drying and carbonation produce mass loss and mass gain
 347 respectively, so they can compensate each other when occurring simultaneously. However, both
 348 phenomena cause negative strain, so their effects overlap in relation with length change. Self-desiccation
 349 is believed not to be causing shrinkage at this period because cement hydration rate after 28 days might
 350 be low in this air-drying curing condition. After 91 days, the tendency changes due to some residual
 351 drying in the absence of further carbonation. At this late period, drying shrinkage seems not to produce a
 352 strong shrinkage.

353 The overlapping of drying and carbonation shrinkage, while respective mass changes compensate each
 354 other, is a visible phenomenon in BCM series too, for the period between 7 and 28 days. Later, mass
 355 starts to increase due to predominance of carbonation over drying. Internally cured mixes show a slightly
 356 higher shrinkage to mass gain ratio after 28 days, as they suffer a higher drying.

357 The presence of MEA has a slight influence on shrinkage to mass ratio so the different substitution rates
 358 show a similar trend for both CM and BCM series.

359 **5.3 Water immersion: unitary water absorption and positive deformation / swelling-expansion**

360 When mortar specimens are immersed in water after demoulding, they continuously absorb water which
 361 can be recorded as mass gain. This mass gain is significant during the first days of immersion, following a
 362 lower rhythm at later ages (**Fig. 13**). Although HPC paste is too dense for an effective external wet
 363 curing, water can still penetrate to a certain depth in water immersion conditions. As specimens under
 364 study have a high surface to volume ratio, water is believed to access a substantial proportion of the
 365 mortar pores. Water gain over time is very similar for all mixes.

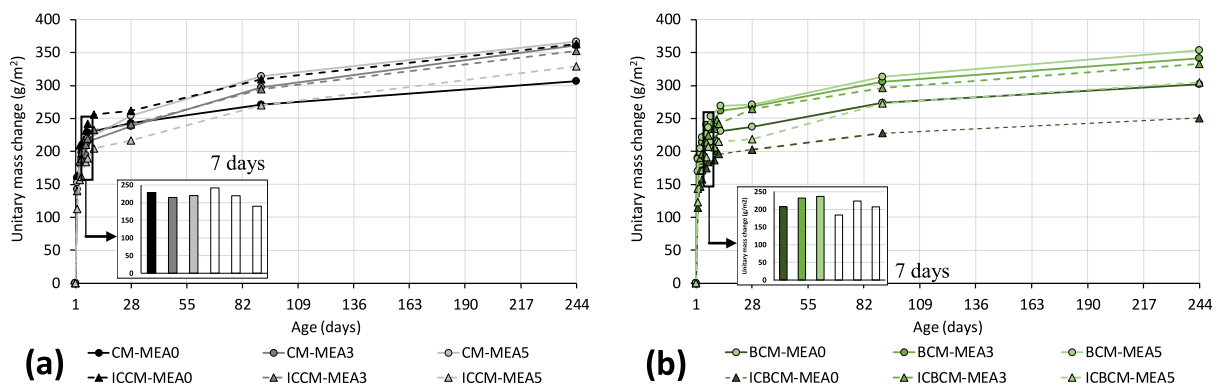


Fig. 13: CM (a) and BCM (b) mass gain (g/dm³).

366 Absorbed water during immersion and interacts with the three different used binders and their reaction
 367 products. Both phenomena contribute to continuous volume increase in all specimens (**Fig. 14**). Along
 368 time, all mixes maintain their relative position from the one with the highest deformation to the one with
 369 the lowest.

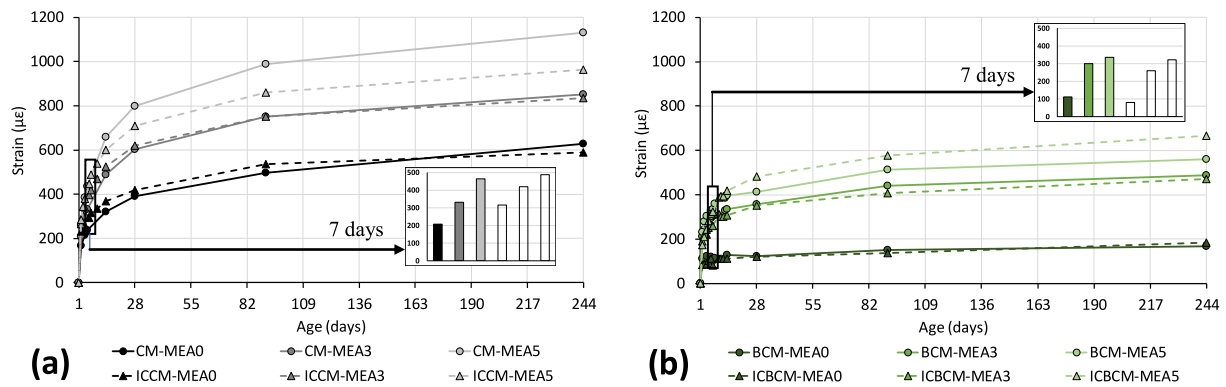


Fig. 14: CM (a) and BCM (b) swelling and expansion [$\mu\epsilon$].

370 In general, the volume increase is more remarkable in CM than in BCM series, although their water gains
 371 are very similar. The principal reason might be the formation of C-S-H and a higher amount of primary
 372 ettringite, both cement hydration products. Ettringite is very porous (its structure is needle-like) and
 373 occupies more volume than involved reactants, so an expansion occurs when it forms [8]. Moreover,
 374 ettringite is able to adsorb big amounts of water causing associated expansion. The expansion due to C-S-
 375 H formation at a porous material scale is a recent approach proposed by [10,11]. Furthermore, negligible
 376 self-desiccation may occur in small specimens subjected to this curing condition, so no internal curing
 377 effect or MEA expansion enhancement is visible.

378 As expected, the more the MEA the more the expansion due to its effective hydration in this curing
 379 condition. This higher MEA expansion is observed in CM and BCM series, but it is proportionally higher
 380 in the second. For example, at 244 days, CM-MEA3 and CM-MEA5 show a deformation 1.35 and 1.80
 381 times CM, while BCM-MEA3 and BCM-MEA5 show a deformation 2.65 and 3.04 times BCM. When
 382 MEA substitutes cement, it reduces the amount of C-S-H and ettringite and their commented associated
 383 expansion, so an expansion is replaced by another one and the difference between them is not drastic. On
 384 the other hand, when MEA substitutes fly ash, no OPC related expansion is avoided and they simply add
 385 up.

386 The relation between water absorption and specimens deformation follows a quadratic tendency (**Fig. 15**).
 387 The continuous expansion of MEA and OPC hydration products makes the pore network volume to
 388 decrease, letting less space for new products growth. This progressive lack of space for free expansions in

389 pores produce stronger tensions and associated external volume increase. This argument has been used by
 390 other authors to explain other expansive phenomena such as those related to delayed ettringite formation
 391 [79].

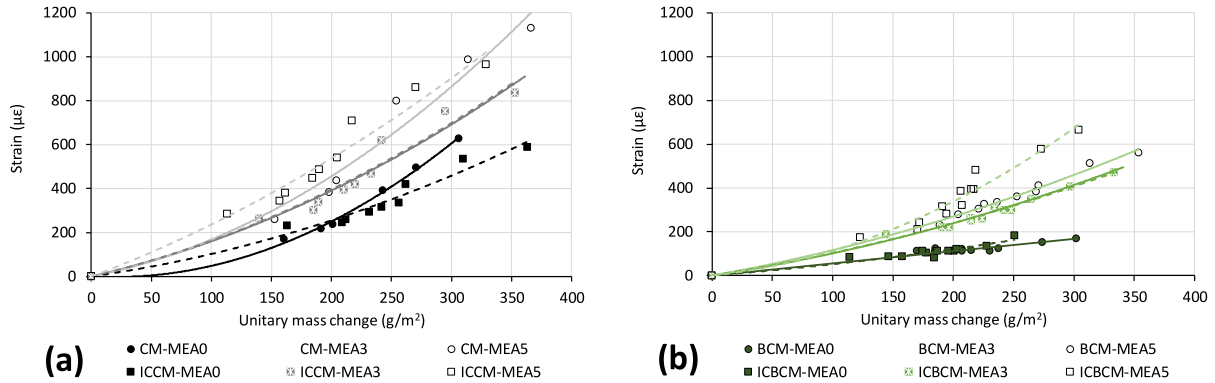


Fig. 15: CM (a) and BCM (b) deformation ($\mu\epsilon$) for corresponding unitary mass gain (g/m^2).

392 CM series shows higher length increase for the same mass gain because the principal causes of expansion
 393 are related to cement hydration. Mixes with MEA register a higher expansion to water gain ratio. For
 394 instance: CM, CM-MEA3 and CM-MEA5 specimens increase their length by 2.05, 2.36 and 3.09
 395 $\mu\epsilon/(g/m^2)$ after 244 days. As water penetrates the mortar, at the same rhythm independent on MEA
 396 content, it interacts with the different binders, hydrating MEA if present.

397 6. Effect of curing conditions on real applications

398 Three curing conditions have been used in this study: sealed, air-drying and water immersion. They have
 399 been chosen because of their correspondence with the standard UNE 80112 [74] and because of their
 400 similarity with some real field curing conditions. The correspondence between laboratory and real field
 401 curing conditions is established taking into account the fundamental differences between laboratory
 402 specimens and construction elements. These differences are related to size and geometry. Laboratory
 403 specimens used in this study are smaller and have a much higher surface to volume ratio than a
 404 construction element such as a standard building beam (Table 7).

405

406

Table 7: Comparison between the geometry of a laboratory specimen and a structural concrete element.

	Length (cm)	High (cm)	Width (cm)	Surface (cm ²)	Volume (cm ³)	Surface/Volume (cm ⁻¹)
Laboratory specimen*	30.0	2.5	2.5	312.5	187.5	1.67
Ordinary building beam**	360	30	20	37200	216000	0.17

*Laboratory standard specimen for length change measurement according to UNE 80112 [74].

**Ordinary building beam according to [80]

407
 408 Environmental conditions affect any element from its surface. Therefore, elements with a high surface to
 409 volume ratio, as it is the case of small laboratory specimens, get proportionally more affected by
 410 surrounding conditions than a construction element for the same level of exposure (**Fig. 16**).

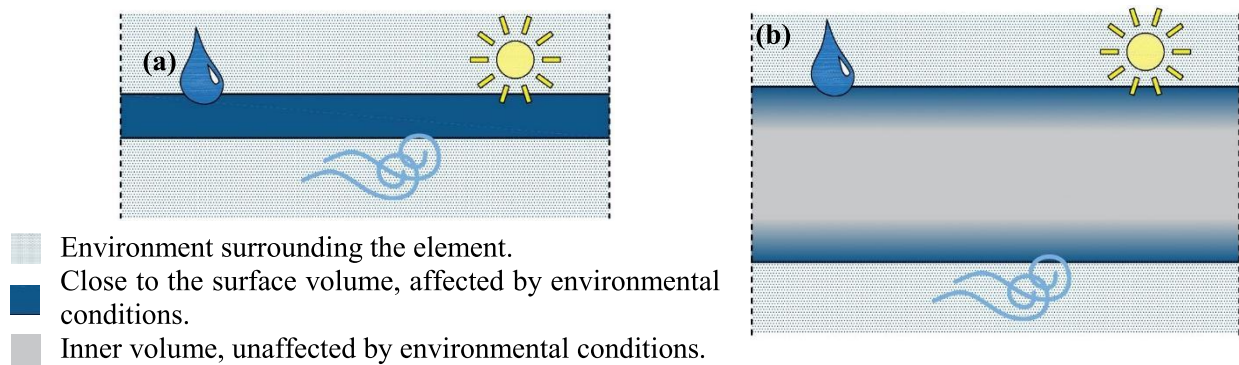


Fig. 16: Influence of environmental conditions on different concrete elements: (a) small laboratory specimen and (b) construction element.

411 A real construction element can be continuously wetted or isolated from environmental humidity changes
 412 by covering it with burlaps, plastic sheets or hydrophobic substances (**Fig. 17**). If this is the case, it can be
 413 considered to perform as a sealed laboratory specimen.



(a)



(b)

Fig. 17: External wet curing **(a)** and covering with burlaps and plastic sheet **(b)**.

414 The absence of curing in field elements can have a similar effect on concrete close-to-surface volume
 415 than air-drying conditions on laboratory specimens. Water immersion can be applied out of the laboratory
 416 to small precast concrete elements. Finally, the non-affected zone of a HPC structural member by
 417 environmental conditions (its inner part) can be considered to performance like laboratory specimens in
 418 sealed conditions [39]. Relationships between analysed curing conditions and field curing conditions are
 419 summarized in **Table 8**.

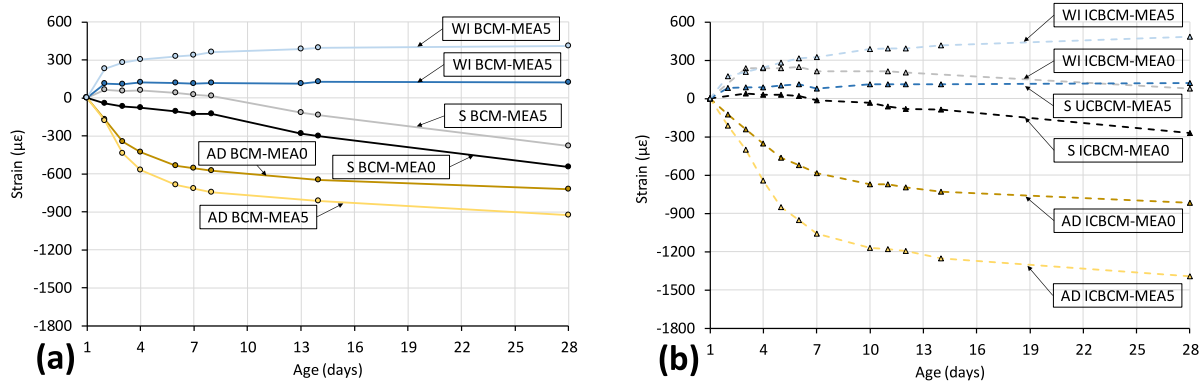
Table 8: Similarity between curing conditions in laboratory and field elements.

Analysed curing conditions	Sealed	Air-drying	Water immersion
Close-to-surface volume of a construction element	Wet external curing or covering	Absence of curing	Water immersion
Inner part of a HPC structural member	Any possible curing condition	-	-

420
 421 In HPC, with a highly dense paste, the inner part can occupy the vast majority of a construction element.
 422 Concrete in similar to sealed conditions is, therefore, the principal contributor to concrete strength, as it
 423 constitutes the most of a hypothetical structural member. This is the reason why compressive strength was
 424 tested on sealed specimens.

425 For each of the three chosen laboratory curing conditions, the effect of three shrinkage mitigation
 426 strategies has been analysed: fly ash as a low reactive supplementary cementitious material, internal
 427 curing and MEA. More than the results analysis carried out in previous paragraphs, results obtained with
 428 different curing conditions can be compared between them (**Fig. 18**). BCM series is chosen for this

429 comparison as the use of blended cement is considered to be recommendable for economic and ecological
 430 reasons over OPC binder. Moreover, only the higher content of MEA (5 %) is presented in order to make
 431 graphs clearer.



WI = Water immersion | S = Sealed | AD = Air-drying

Fig. 18: Effect of the highest dosage of MEA (5 %) over blended cement mixes without (a) and with (b) internal curing, when the three curing conditions are applied.

432 Water immersion leads to expansions whereas air-drying condition lead to the highest values of
 433 shrinkage. Sealed condition lead to lower shrinkage than air-drying, and some mixes show initial
 434 swelling.

435 Following the correspondence between laboratory and real field curing conditions established in previous
 436 paragraphs (**Table 8**), the next can be stated. On the close to surface part of an HPC structural member,
 437 the combination of internal curing and MEA has a negative effect if water evaporation is not prevented
 438 somehow. On the other hand, if water curing is used, what can happen for small precast elements,
 439 undesired expansions on the close to the surface area could happen, being more probable if this kind of
 440 curing is applied for a long time. Finally, if HPC is covered with burlaps, plastic sheet or sealant, and in
 441 the inner part of a construction element whatever curing condition is used, the three shrinkage reduction
 442 strategies used in this study show a positive effect on shrinkage. What is more, internal curing and MEA
 443 show a synergistic effect, having a superior performance together than separately in HPC.

444 Therefore, for internally cured HPC incorporating MEA, it is recommended not to dispense with external
 445 curing and being careful with water immersion curing times. This way, it can be get better advantage of
 446 the combined effect of both shrinkage reduction strategies.

447 **7. Conclusions**

448 The combined effect on high performance concrete (HPC) of three shrinkage reduction strategies: the use
449 of fly ash as a low reactive cementitious material, internal curing via saturated coal bottom ash and
450 magnesium based expansive agent (MEA), has been studied. The following conclusions are drawn:

- 451 - The inclusion of small amounts of MEA (until 5 % of binder) and coal bottom ash as water
452 reservoirs for internal curing (until 30 % of aggregate) in HPC has a slight effect on compressive
453 strength.
- 454 - HPC with low content of water limits MEA expansion, however internal curing can effectively
455 provide the extra water needed for this propose. The synergistic effect of both shrinkage
456 reduction strategies is effective for minimising autogenous shrinkage.
- 457 - If water evaporation is not prevented, the use of both MEA and internal curing separately or
458 together makes shrinkage to increase.
- 459 - MEA effectively expands in water immersed HPC and, in this case, internal curing has no effect
460 over its expansion capacity.
- 461 - In comparison with a conventional HPC with no shrinkage reduction strategies, blended cement
462 HPC with high volume of fly ash, MEA and internal curing presents a much better volume
463 stability and acceptable compressive strength. Negative effects such as a possible higher
464 shrinkage on concrete surface are avoidable by preventing water evaporation with conventional
465 external curing methods.
- 466 - Other low reactive supplementary cementitious materials and other expansive agents could serve
467 to the same propose, and other aggregates could be suitable to work as internal curing water
468 reservoirs. Future research must study some alternative materials that could lead to comparable
469 results.

470 **Acknowledgments**

471 This work has been carried out within the framework of the HACCURACEM project (BIA2017-85657-
472 R), funded by the Ministry of Economy, Industry and Competitiveness, State Program for Research,
473 Development and Innovation aimed at the challenges of Society, within the framework of the State Plan

474 for Scientific and Technical Research and Innovation 2013-2016, Call 2017. We also thank to Ryerson
475 University (Toronto, Canada) in whose facilities the experimental part of this work was developed during
476 a predoctoral stay funded by the government of Galicia, Xunta de Galicia. Finally, we highlight the
477 collaboration of the companies Votorantim Cimentos and Grupo BASF, for the contribution of some of
478 the materials used in this research.

479 **References**

- 480 [1] K. Wang, D.C. Jansen, S.P. Shah, A.F. Karr, Permeability study of cracked concrete, *Cem. Concr.*
481 *Res.* 27 (1997) 381–393.
- 482 [2] L. Wu, N. Farzadnia, C. Shi, Z. Zhang, H. Wang, Autogenous shrinkage of high performance
483 concrete: A review, *Constr. Build. Mater.* 149 (2017) 62–75.
484 doi:10.1016/j.conbuildmat.2017.05.064.
- 485 [3] E. Holt, Contribution of mixture design to chemical and autogenous shrinkage of concrete at early
486 ages, *Cem. Concr. Res.* 35 (2005) 464–472. doi:10.1016/j.cemconres.2004.05.009.
- 487 [4] P. Lura, O.M. Jensen, K. Van Breugel, Autogenous shrinkage in high-performance cement paste :
488 An evaluation of basic mechanisms Modeling of autogenous relative humidity change and
489 autogenous, *Cem. Concr. Res.* 33 (2003) 223–232. [https://ac.els-cdn.com/S0008884602008906/1-](https://ac.els-cdn.com/S0008884602008906/1-s2.0-S0008884602008906-main.pdf?_tid=9c61cc0a-d05d-11e7-87d7-00000aacb35d&acdnat=1511448793_2774e5b1adbc8f1a919776d1ca54c419)
490 [s2.0-S0008884602008906-main.pdf?_tid=9c61cc0a-d05d-11e7-87d7-](https://ac.els-cdn.com/S0008884602008906-main.pdf?_tid=9c61cc0a-d05d-11e7-87d7-00000aacb35d&acdnat=1511448793_2774e5b1adbc8f1a919776d1ca54c419)
491 [00000aacb35d&acdnat=1511448793_2774e5b1adbc8f1a919776d1ca54c419.](https://ac.els-cdn.com/S0008884602008906-main.pdf?_tid=9c61cc0a-d05d-11e7-87d7-00000aacb35d&acdnat=1511448793_2774e5b1adbc8f1a919776d1ca54c419)
- 492 [5] B. Persson, Experimental studies on shrinkage of high-performance concrete, *Cem. Concr. Res.* 28
493 (1998) 1023–1036. doi:10.1016/S0008-8846(98)00068-4.
- 494 [6] V. Baroghel-Bouny, P. Mounanga, A. Khelidj, A. Loukili, N. Rafai, Autogenous deformations of
495 cement pastes: Part II. W/C effects, micro-macro correlations, and threshold values, *Cem. Concr.*
496 *Res.* 36 (2006) 123–136. doi:10.1016/j.cemconres.2004.10.020.
- 497 [7] Z. Jiang, Z. Sun, P. Wang, Autogenous relative humidity change and autogenous shrinkage of
498 high-performance cement pastes, *Cem. Concr. Res.* 35 (2005) 1539–1545.
499 doi:10.1016/j.cemconres.2004.06.028.
- 500 [8] J. Carette, S. Joseph, Ö. Cizer, S. Staquet, Decoupling the autogenous swelling from the self-
501 desiccation deformation in early age concrete with mineral additions: Micro-macro observations
502 and unified modelling, *Cem. Concr. Compos.* 85 (2018) 122–132.
503 doi:10.1016/j.cemconcomp.2017.10.008.
- 45 504 [9] E. Tazawa, S. Miyazawa, T. Kasai, Chemical Shrinkage and Autogenous Shrinkage of Hydrating
46 505 Cement Paste, *Cem. Concr. Res.* 25 (1995) 288–292.
- 47
48 506 [10] S. Rahimi-Aghdam, Z.P. Bažant, M.J. Abdolhosseini Qomi, Cement hydration from hours to
49 507 centuries controlled by diffusion through barrier shells of C-S-H, *J. Mech. Phys. Solids.* 99 (2017)
50 508 211–224. doi:10.1016/j.jmps.2016.10.010.
- 51
52 509 [11] S. Rahimi-Aghdam, E. Masoero, M. Rasoolinejad, Z.P. Bažant, Century-long expansion of
53 510 hydrating cement counteracting concrete shrinkage due to humidity drop from selfdesiccation or
54 511 external drying, *Mater. Struct. Constr.* 52 (2019). doi:10.1617/s11527-018-1307-8.
- 55
56 512 [12] L. Barcelo, M. Moranville, B. Clavaud, Autogenous shrinkage of concrete: A balance between
57 513 autogenous swelling and self-desiccation, *Cem. Concr. Res.* 35 (2005) 177–183.
58 514 doi:10.1016/j.cemconres.2004.05.050.
- 59
60 515 [13] E. Marušić, N. Štirmer, Autogenous Shrinkage and Expansion Related to Compressive Strength

- 516 and Concrete Composition, *J. Adv. Concr. Technol.* 14 (2016) 489–501. doi:10.3151/jact.14.489.
- 517 [14] M. Vinkler, J.L. Vitek, Drying shrinkage of concrete elements, *Struct. Concr.* 18 (2017) 92–103.
518 doi:10.1002/suco.201500208.
- 519 [15] J. Zhang, D. Hou, Y. Gao, Integrative Studies on Autogenous and Drying Shrinkages of Concrete
520 at Early-Age, *Adv. Struct. Eng.* 15 (2012) 1041–1051. doi:10.1260/1369-4332.15.7.1041.
- 521 [16] X. Hu, Z. Shi, C. Shi, Z. Wu, B. Tong, Z. Ou, G. de Schutter, Drying shrinkage and cracking
522 resistance of concrete made with ternary cementitious components, *Constr. Build. Mater.* 149
523 (2017) 406–415. doi:10.1016/j.conbuildmat.2017.05.113.
- 524 [17] J. Yang, Q. Wang, Y. Zhou, Influence of Curing Time on the Drying Shrinkage of Concretes with
525 Different Binders and Water-to-Binder Ratios, *Adv. Mater. Sci. Eng.* 2017 (2017) 1–10.
526 doi:10.1155/2017/2695435.
- 527 [18] M. Ba, C. Qian, H. Wang, Effects of specimen shape and size on water loss and drying shrinkage
528 of cement-based materials, *J. Wuhan Univ. Technol. Mater. Sci. Ed.* 28 (2013) 733–740.
529 doi:10.1007/s11595-013-0761-y.
- 530 [19] J. Liu, N. Farzadnia, C. Shi, X. Ma, Effects of superabsorbent polymer on shrinkage properties of
531 ultra-high strength concrete under drying condition, *Constr. Build. Mater.* 215 (2019) 799–811.
532 doi:10.1016/j.conbuildmat.2019.04.237.
- 533 [20] A. Dönmez, Z.P. Bažant, Shape factors for concrete shrinkage and drying creep in model B4
534 refined by nonlinear diffusion analysis, *Mater. Struct. Constr.* 49 (2016) 4779–4784.
535 doi:10.1617/s11527-016-0824-6.
- 536 [21] B. Šavija, M. Luković, Carbonation of cement paste: Understanding, challenges, and
537 opportunities, *Constr. Build. Mater.* 117 (2016) 285–301. doi:10.1016/j.conbuildmat.2016.04.138.
- 538 [22] I. Mehdipour, K.H. Khayat, Elucidating the Role of Supplementary Cementitious Materials on
539 Shrinkage and Restrained-Shrinkage Cracking of Flowable Eco-Concrete, *J. Mater. Civ. Eng.* 30
540 (2017) 04017308. doi:10.1061/(asce)mt.1943-5533.0002191.
- 541 [23] B.I. Yoshitake, H. Wong, T. Ishida, A.Y. Nassif, Thermal stress of high volume fly-ash (HVFA)
542 concrete made with limestone aggregate, *Constr. Build. Mater.* 71 (2014) 216–225.
543 doi:10.1016/j.conbuildmat.2014.08.028.
- 544 [24] E. Ghafari, S.A. Ghahari, H. Costa, E. Júlio, A. Portugal, L. Durães, Effect of supplementary
545 cementitious materials on autogenous shrinkage of ultra-high performance concrete, *Constr. Build.*
546 *Mater.* 127 (2016) 43–48. doi:10.1016/j.conbuildmat.2016.09.123.
- 547 [25] Y. Akkaya, C. Ouyang, S.P. Shah, Effect of supplementary cementitious materials on shrinkage
548 and crack development in concrete, *Cem. Concr. Compos.* 29 (2007) 117–123.
549 doi:10.1016/j.cemconcomp.2006.10.003.
- 45 550 [26] P. Saiz-Martínez, D. Ferrández-Vega, C. Morón-Fernández, A. Payán De Tejada-Alonso,
46 551 Comparative study of the influence of three types of fibre in the shrinkage of recycled mortar,
47 552 *Mater. Constr.* 68 (2018) 1–12. doi:10.3989/mc.2018.07817.
- 48 553 [27] K. Huang, M. Deng, L. Mo, Y. Wang, Early age stability of concrete pavement by using hybrid
49 554 fiber together with MgO expansion agent in high altitude locality, *Constr. Build. Mater.* 48 (2013)
50 555 685–690. doi:10.1016/j.conbuildmat.2013.07.089.
- 52 556 [28] Q. Cao, Y. Cheng, M. Cao, Q. Gao, Workability, strength and shrinkage of fiber reinforced
53 557 expansive self-consolidating concrete, *Constr. Build. Mater.* 131 (2017) 178–185.
54 558 doi:10.1016/j.conbuildmat.2016.11.076.
- 56 559 [29] D.M. Al Saffar, A.J.K. Al Saad, B.A. Tayeh, Effect of internal curing on behavior of high
57 560 performance concrete: An overview, *Case Stud. Constr. Mater.* 10 (2019) e00229.
58 561 doi:10.1016/j.cscm.2019.e00229.
- 60 562 [30] O.M. Jensen, P. Lura, Techniques and materials for internal water curing of concrete, *Mater.*

- 563 Struct. Constr. 39 (2006) 817–825. doi:10.1617/s11527-006-9136-6.
- 564 [31] D.P. Bentz, P. Lura, J.W. Roberts, Mixture Proportioning for Internal Curing, *Concr. Int.* 27
565 (2005) 35–40.
- 566 [32] S. Seara-Paz, B. González-Fonteboa, F. Martínez-Abella, I. González-Taboada, Time-dependent
567 behaviour of structural concrete made with recycled coarse aggregates. Creep and shrinkage,
568 *Constr. Build. Mater.* 122 (2016) 95–109. doi:10.1016/j.conbuildmat.2016.06.050.
- 569 [33] P. min Zhan, Z. hai He, Application of shrinkage reducing admixture in concrete: A review,
570 *Constr. Build. Mater.* 201 (2019) 676–690. doi:10.1016/j.conbuildmat.2018.12.209.
- 571 [34] W. Zuo, P. Feng, P. Zhong, Q. Tian, J. Liu, W. She, Effects of a novel polymer-type shrinkage-
572 reducing admixture on early age microstructure evolution and transport properties of cement
573 pastes, *Cem. Concr. Compos.* 95 (2019) 33–41. doi:10.1016/j.cemconcomp.2018.10.011.
- 574 [35] D.P. Bentz, M.R. Geiker, K.K. Hansen, Shrinkage-reducing admixtures and early-age desiccation
575 in cement pastes and mortars, *Cem. Concr. Res.* 31 (2001) 1075–1085. doi:10.1016/S0008-
576 8846(01)00519-1.
- 577 [36] M. Valipour, K.H. Khayat, Coupled effect of shrinkage-mitigating admixtures and saturated
578 lightweight sand on shrinkage of UHPC for overlay applications, *Constr. Build. Mater.* 184 (2018)
579 320–329. doi:10.1016/j.conbuildmat.2018.06.191.
- 580 [37] K. Liu, Z. Shui, T. Sun, G. Ling, X. Li, S. Cheng, Effects of combined expansive agents and
581 supplementary cementitious materials on the mechanical properties, shrinkage and chloride
582 penetration of self-compacting concrete, *Constr. Build. Mater.* 211 (2019) 120–129.
583 doi:10.1016/j.conbuildmat.2019.03.143.
- 584 [38] M.S. Meddah, M. Suzuki, R. Sato, Influence of a combination of expansive and shrinkage-
585 reducing admixture on autogenous deformation and self-stress of silica fume high-performance
586 concrete, *Constr. Build. Mater.* 25 (2011) 239–250. doi:10.1016/j.conbuildmat.2010.06.033.
- 587 [39] K. Kovler, S. Zhutovsky, Overview and future trends of shrinkage research, *Mater. Struct. Constr.*
588 39 (2006) 827–847. doi:10.1617/s11527-006-9114-z.
- 589 [40] G. Zhang, G. Li, Effects of mineral admixtures and additional gypsum on the expansion
590 performance of sulphoaluminate expansive agent at simulation of mass concrete environment,
591 *Constr. Build. Mater.* 113 (2016) 970–978. doi:10.1016/j.conbuildmat.2016.03.131.
- 592 [41] P. Yan, X. Qin, The effect of expansive agent and possibility of delayed ettringite formation in
593 shrinkage-compensating massive concrete, *Cem. Concr. Res.* 31 (2001) 335–337.
594 doi:10.1016/S0008-8846(00)00453-1.
- 595 [42] F. Tittarelli, C. Giosuè, S. Monosi, Combined Use of Shrinkage Reducing Admixture and CaO in
596 Cement Based Materials, *IOP Conf. Ser. Mater. Sci. Eng.* 245 (2017). doi:10.1088/1757-
597 899X/245/2/022093.
- 598 [43] V. Corinaldesi, Combined effect of expansive, shrinkage reducing and hydrophobic admixtures for
599 durable self compacting concrete, *Constr. Build. Mater.* 36 (2012) 758–764.
600 doi:10.1016/j.conbuildmat.2012.04.129.
- 601 [44] M. Collepardi, A. Borsoi, S. Collepardi, J.J. Ogoumah Olagot, R. Troli, Effects of shrinkage
602 reducing admixture in shrinkage compensating concrete under non-wet curing conditions, *Cem.*
603 *Concr. Compos.* 27 (2005) 704–708. doi:10.1016/j.cemconcomp.2004.09.020.
- 604 [45] M. Collepardi, R. Troli, M. Bressan, F. Liberatore, G. Sforza, Crack-free concrete for outside
605 industrial floors in the absence of wet curing and contraction joints, *Cem. Concr. Compos.* 30
606 (2008) 887–891. doi:10.1016/j.cemconcomp.2008.07.002.
- 607 [46] C. Maltese, C. Pistolesi, A. Lolli, A. Bravo, T. Cerulli, D. Salvioni, Combined effect of expansive
608 and shrinkage reducing admixtures to obtain stable and durable mortars, *Cem. Concr. Res.* 35
609 (2005) 2244–2251. doi:10.1016/j.cemconres.2004.11.021.

- 610 [47] V. Corinaldesi, J. Donnini, A. Nardinocchi, The influence of calcium oxide addition on properties
611 of fiber reinforced cement-based composites, *J. Build. Eng.* 4 (2015) 14–20.
612 doi:10.1016/j.jobbe.2015.07.009.
- 613 [48] Q. Cao, Z.J. Ma, Structural behavior of FRP enclosed shrinkage-compensating concrete (SHCC)
614 beams made with different expansive agents, *Constr. Build. Mater.* 75 (2015) 450–457.
615 doi:10.1016/j.conbuildmat.2014.11.045.
- 616 [49] W. Sun, H. Chen, X. Luo, H. Qian, The effect of hybrid fibers and expansive agent on the
617 shrinkage and permeability of high-performance concrete, *Cem. Concr. Res.* 31 (2001) 595–601.
618 doi:10.1016/S0008-8846(00)00479-8.
- 619 [50] S. Nagataki, H. Gomi, Expansive admixtures (mainly ettringite), *Cem. Concr. Compos.* 20 (1998)
620 163–170. doi:10.1016/s0958-9465(97)00064-4.
- 621 [51] C. S., Mechanism of expansion of concrete due to the presence of dead-burnt CaO and MgO.,
622 *Cem. Concr. Res.* 25 (1995) 51–56.
- 623 [52] M.A.A. Sherir, K.M.A. Hossain, M. Lachemi, Self-healing and expansion characteristics of
624 cementitious composites with high volume fly ash and MgO-type expansive agent, *Constr. Build.*
625 *Mater.* 127 (2016) 80–92. doi:10.1016/j.conbuildmat.2016.09.125.
- 626 [53] L. Mo, M. Liu, A. Al-Tabbaa, M. Deng, Deformation and mechanical properties of the expansive
627 cements produced by inter-grinding cement clinker and MgOs with various reactivities, *Constr.*
628 *Build. Mater.* 80 (2015) 1–8. doi:10.1016/j.conbuildmat.2015.01.066.
- 629 [54] R. Polat, R. Demirboğa, W.H. Khushefati, Effects of nano and micro size of CaO and MgO, nano-
630 clay and expanded perlite aggregate on the autogenous shrinkage of mortar, *Constr. Build. Mater.*
631 81 (2015) 268–275. doi:10.1016/j.conbuildmat.2015.02.032.
- 632 [55] H. Li, Q. Tian, H. Zhao, A. Lu, J. Liu, Temperature sensitivity of MgO expansive agent and its
633 application in temperature crack mitigation in shiplock mass concrete, *Constr. Build. Mater.* 170
634 (2018) 613–618. doi:10.1016/j.conbuildmat.2018.02.184.
- 635 [56] V.C. Nguyen, F.G. Tong, V.N. Nguyen, Modeling of autogenous volume deformation process of
636 RCC mixed with MgO based on concrete expansion experiment, *Constr. Build. Mater.* 210 (2019)
637 650–659. doi:10.1016/j.conbuildmat.2019.03.226.
- 638 [57] L. Yu, M. Deng, L. Mo, J. Liu, F. Jiang, Effects of Lightly Burnt MgO Expansive Agent on the
639 Deformation and Microstructure of Reinforced Concrete Wall, *Adv. Mater. Sci. Eng.* 2019 (2019)
640 1–9. doi:10.1155/2019/1948123.
- 641 [58] M.A.A. Sherir, K.M.A. Hossain, M. Lachemi, Development and recovery of mechanical
642 properties of self-healing cementitious composites with MgO expansive agent, *Constr. Build.*
643 *Mater.* 148 (2017) 789–810. doi:10.1016/j.conbuildmat.2017.05.063.
- 644 [59] M.A.A. Sherir, K.M.A. Hossain, M. Lachemi, The influence of MgO-type expansive agent
645 incorporated in self-healing system of Engineered cementitious Composites, *Constr. Build. Mater.*
646 149 (2017) 164–185. doi:10.1016/j.conbuildmat.2017.05.109.
- 647 [60] J.A. Mejias, A.J. Berry, K. Refson, D.G. Fraser, The kinetics and mechanism of MgO dissolution,
648 *Chem. Phys. Lett.* 314 (1999) 558–563. doi:10.1007/BF00551026.
- 649 [61] D. Chongjiang, A Review of Magnesium Oxide in Concrete, *Concr. Int.* (2005) 45–50.
- 650 [62] P. Gao, X. Lu, F. Geng, X. Li, J. Hou, H. Lin, N. Shi, Production of MgO-type expansive agent in
651 dam concrete by use of industrial by-products, *Build. Environ.* 43 (2008) 453–457.
652 doi:10.1016/j.buildenv.2007.01.037.
- 653 [63] T. I. Akin Altun(Department of Metallurgical and Materials Engineering, Dokuz Eylul University,
654 35100, Bornova-Izmir, T. Ismail Yilmaz(Filyos Refractories, Hisaronu-Zonguldak, Study on steel
655 furnace slags with high MgO as additive in Portland cement, *Cem. Concr. Res.* 32 (2002) 1247–
656 1249.

- 657 [64] X. Lingling, D. Min, Dolomite used as raw material to produce MgO-based expansive agent, *Cem. Concr. Res.* 35 (2005) 1480–1485. doi:10.1016/j.cemconres.2004.09.026.
658
- 659 [65] S.W. Choi, B.S. Jang, J.H. Kim, K.M. Lee, Durability characteristics of fly ash concrete
660 containing lightly-burnt MgO, *Constr. Build. Mater.* 58 (2014) 77–84.
661 doi:10.1016/j.conbuildmat.2014.01.080.
- 662 [66] P.W. Gao, S.Y. Xu, X. Chen, J. Li, X.L. Lu, Research on autogenous volume deformation of
663 concrete with MgO, *Constr. Build. Mater.* 40 (2013) 998–1001.
664 doi:10.1016/j.conbuildmat.2012.11.025.
- 665 [67] A. Wang, M. Deng, D. Sun, L. Mo, J. Wang, M. Tang, Effect of combination of steel fiber and
666 mgo-type expansive agent on properties of concrete, *J. Wuhan Univ. Technol. Mater. Sci. Ed.* 26
667 (2011) 786–790. doi:10.1007/s11595-011-0311-4.
- 668 [68] X. Chen, H.Q. Yang, W.W. Li, Factors analysis on autogenous volume deformation of MgO
669 concrete and early thermal cracking evaluation, *Constr. Build. Mater.* 118 (2016) 276–285.
670 doi:10.1016/j.conbuildmat.2016.02.093.
- 671 [69] F. Li, Y. Chen, S. Long, Influence of MgO Expansive agent on behaviour of cement pastes and
672 concrete, *Arab. J. Sci. Eng.* 35 (2010) 125–139.
- 673 [70] M. Liwu, D. Ming, T. Mingshu, A.-T. Abir, MgO expansive cement and concrete in China: Past,
674 present and future, *Cem. Concr. Res.* 57 (2014) 1–12.
- 675 [71] American Society for Testing and Materials, ASTM C1761: Lightweight Aggregate for Internal
676 Curing of Concrete, (n.d.). doi:10.1520/C1761.
- 677 [72] D.P. Bentz, K.A. Snyder, Protected paste volume in concrete, *Cem. Concr. Res.* 29 (2002) 1863–
678 1867. doi:10.1016/s0008-8846(99)00178-7.
- 679 [73] L. Mo, M. Deng, M. Tang, Effects of calcination condition on expansion property of MgO-type
680 expansive agent used in cement-based materials, *Cem. Concr. Res.* 40 (2010) 437–446.
681 doi:10.1016/j.cemconres.2009.09.025.
- 682 [74] AENOR, UNE 80112 Métodos de ensayo de cementos. Ensayos físicos. Determinación de la
683 retracción de secado y del hinchamiento en agua., (2016).
- 684 [75] AENOR, UNE-EN 16322 Conservation of Cultural Heritage. Test methods. Determination of
685 drying properties., 2016.
- 686 [76] V. Shah, S. Bishnoi, Carbonation resistance of cements containing supplementary cementitious
687 materials and its relation to various parameters of concrete, *Constr. Build. Mater.* 178 (2018) 219–
688 232. doi:10.1016/j.conbuildmat.2018.05.162.
- 689 [77] H. Ye, Mitigation of Drying and Carbonation Shrinkage of Cement Paste using Magnesia, *J. Adv.
690 Concr. Technol.* 16 (2018) 476–484. doi:10.3151/jact.16.476.
- 691 [78] B. Persson, Eight-year exploration of shrinkage in high-performance concrete, *Cem. Concr. Res.*
692 32 (2002) 1229–1237. doi:10.1016/S0008-8846(02)00764-0.
- 693 [79] H.F.W. Taylor, C. Famy, K.L. Scrivener, Delayed ettringite formation, *Cem. Concr. Res.* 31
694 (2001) 683–693. doi:10.1016/S0008-8846(01)00466-5.
- 695 [80] S. Seara-Paz, B. González-Fonteboa, F. Martínez-Abella, D. Carro-López, Long-term flexural
696 performance of reinforced concrete beams with recycled coarse aggregates, *Constr. Build. Mater.*
697 176 (2018) 593–607. doi:10.1016/j.conbuildmat.2018.05.069.
- 698